

High-Gradient-Doped Strained GaAsP

A. Brachmann, D. Luh, and T. Maruyama

Introduction

The NLC is presently designed to operate with a train of 190 micro-bunches, spaced 1.4 ns apart (total of 266 ns), and each micro-bunch is required to have as much as 1.4×10^{10} e- per pulse in 0.5 ns (full width) at the gun, totaling 2.7×10^{12} e- per train [1]. The factor limiting the photoemission of high electron current is the surface photovoltage effect, and a typical SLC strained photocathode (100-nm strained GaAs with a medium doping level of $5 \times 10^{18} \text{ cm}^{-3}$) saturates at the level of 8×10^{11} e- for a 300-ns pulse. A recent study shows that the surface photovoltage build-up can be reduced significantly by increasing the doping concentration to at least $2 \times 10^{19} \text{ cm}^{-3}$ [2]. However, increasing the doping level leads to depolarization of the electron spin. To increase the doping level without spin de-polarization, a high gradient doping technique has been explored [3]. The active layer is doped at $5 \times 10^{17} \text{ cm}^{-3}$ with a 10-nm surface layer doped at $5 \times 10^{19} \text{ cm}^{-3}$. The lower-than-standard doping level in the active layer achieves high polarization, while the high surface doping solves the charge limit problem.

The high gradient doping technique was first applied to the strained GaAs structure. While no charge limit behavior was observed, the quantum efficiency (QE) was about a factor of two lower than for typical strained GaAs. Because of the high gradient doping, an energy barrier was expected to develop in the conduction band (see Figure 1(a)), and the lower than average QE might be due to this barrier. To prevent such an energy barrier, the active layer was changed to $\text{GaAs}_{0.95}\text{P}_{0.05}$ which raised the conduction band energy to compensate for the energy difference from the gradient doping (see Figure 1(b)). This tech note describes recent charge measurements from the high-gradient-doped strained GaAsP made at the SLAC Gun Test Lab (GTL).

Photocathode

Figure 2 shows the photocathode structure of Bandwidth Semiconductor Inc. #M05-5868. The active layer is $\text{GaAs}_{0.95}\text{P}_{0.05}$ with a doping level of $5 \times 10^{17} \text{ cm}^{-3}$ and a 10-nm GaAs surface doped at $5 \times 10^{19} \text{ cm}^{-3}$. The 2" wafer as received was anodized at 2.5 V, forming a 3.5-nm oxide layer at the surface for protection.

The QE and polarization measured at low voltage in the Cathode Test Lab. (CTL) are shown in Figure 3. A QE of 0.2% and peak polarization of 80% were measured at room temperature. The wavelength at the peak polarization was about 805 nm. The 40-nm blue shift with respect to a standard strained GaAs cathode is due to the larger band gap energy of the $\text{GaAs}_{0.95}\text{P}_{0.05}$ active layer.

Laser System

The flashlamp-pumped Ti:Sapphire laser (Flash-Ti) produced a 10- μs long pulse as shown in Figure 4. To produce a pulse equivalent to one NLC train, a 300-ns long pulse was sliced out of the 10- μs pulse using a crossed-polarizer pair and a Pockels cell. When a pulse was sliced at $t \sim 7.5 \mu\text{s}$ ("Slice 1" in Figure 4), the pulse had a flat top shape, but the maximum energy was limited to 100 $\mu\text{J}/\text{pulse}$. To increase the energy, a pulse was also sliced at $t \sim 1.5 \mu\text{s}$ ("Slice 2" in Figure 4). The maximum laser energy increased to 300 $\mu\text{J}/\text{pulse}$ with a temporal pulse shape shown in Figure 5.

An additional polarizer and a Pockels cell were used to control the laser intensity. The wavelength of the laser was set by a retardation plate at a Brewster angle.

The YAG-pumped Ti:Sapphire laser (YAG-Ti) produced a 4-ns long pulse as shown in Figure 6. The slicer that produces a 2-ns pulse and the intensity controller were bypassed for this experiment. The laser energy was about 20 $\mu\text{J}/\text{pulse}$.

Since we did not have a laser system capable of producing the NLC multi-bunch structure, we simulated the NLC beam condition using the Flash-Ti and YAG-Ti laser systems. A Flash-Ti pulse was equivalent to one NLC train without the multi-bunch structure. However, the Flash-Ti pulse alone did not produce the NLC peak current, 9 A ($= 1.4 \times 10^{10}$ e- in 0.25 ns FWHM). In order to test the peak current capability, the YAG-Ti pulse was overlaid on the Flash-Ti pulse.

The Flash-Ti laser was set to 804 nm throughout the charge measurements. However, the YAG-Ti laser was found not to lase at 804 nm. The “850 nm” mirror set lased at longer than 817 nm while the “765 nm” mirror set at shorter than 790 nm. Therefore, the YAG-Ti laser was set at 780 nm

The laser spot size on the cathode was varied by a telescope, and the laser beam spatial profile was analyzed by a CCD camera. Figure 7(a) and 7(b) show the beam profiles of Flash:Ti and YAG:Ti lasers, respectively. As seen from the figures, both lasers were multi-mode.

Gun System in GTL

A 22.5-mm diameter cathode was cut from the wafer. After degreasing in boiling trichloroethane, the anodized layer was stripped in ammonium hydroxide. The cathode was activated twice in the GTL Load-Lock following the standard heat-cleaning and activation process (heat cleaning at 600°C for 1 hour and cesium+NF₃ co-adsorption). The QEs at 670 nm during the activations were 4.6% (1st) and 5.3% (2nd). The QE decreased by about 10% ($\delta\text{QE}/\text{QE}$) a day, and the cathode was cesiated every third day. Over six weeks the QE variations and cesiations were reproducible. The gun was operated at -120 kV with the cathode held at 0° C. The dark current was typically 35 - 40 nA.

An optically isolated nano-ammeter was used to measure the average photoemission current, and a fast Faraday cup with a time resolution of 0.5 ns was used to measure the temporal beam profile.

Results

Figure 8 shows the polarization as a function of wavelength. The peak polarization was 78.5% at 804 nm.

Figure 9 shows representative temporal profiles of the emission current pulses measured using varying Flash-Ti laser energies. The laser pulse was sliced at “Slice 1” in Figure 4. As the laser energy was increased, the temporal profile simply scaled without developing the leading edge spike typically observed in the charge-limited photoemission. Figure 10 shows the charge output as a function of the laser energy. The charge output was linear up to the max. laser energy.

Since the charge output was limited by the laser energy, we changed the slice timing to “Slice 2” in Figure 4, and we also increased the photon density by reducing the laser spot size. However, as the

laser spot size was reduced, the photoemission would be influenced by the space charge limit of the gun. Figure 11 (a) and 11 (b) show the charge output as a function of the laser spot size for the Flash-Ti and YAG-Ti, respectively. Figure 12 shows the expected space-charge-limited emission as a function of the laser spot size using the space charge limit of 15 A from a 2 cm diameter laser spot at 120 kV. With a spot size larger than about 10 mm for Flash-Ti and about 14 mm for YAG-Ti, the charge output was limited by the laser energy. As the laser spot size was reduced, the charge output decreased due to the space charge limit. Since the lasers are multi-mode as shown in Figure 7, it is not straightforward to compare these results. The best operating diameter for achieving the highest photon density was about 14 mm where the photoemission was not affected by the space charge limit.

The laser spot size of both lasers was set to 14 mm, and the Flash-Ti pulse length was set to 270 ns. The charge output was measured as a function of the Flash-Ti laser energy. Then, the YAG-Ti laser was overlaid on the Flash-Ti laser. While the YAG-Ti laser energy was fixed at 20 $\mu\text{J}/\text{pulse}$, the charge output was measured as the Flash-Ti laser energy was increased. Figure 13 shows the charge output as a function of the Flash-Ti laser energy with and without the YAG-Ti laser. The YAG-Ti laser by itself produced 2.3×10^{11} e-/pulse, equivalent to 9.2 A peak current (assuming a Gaussian pulse). The charge output was again linear up the max. laser energy, producing a max. charge of 2.2×10^{12} e- in 270 ns. If we can assume the spot size scaling, this charge is equivalent to 4.5×10^{12} e- from a 20-mm diameter cathode.

Conclusions

The charge capabilities of a high gradient doped strained GaAsP have been tested. A charge as large as 2.2×10^{12} e- was produced from a 14-mm diameter in 270 ns. By overlaying a short pulse laser, the peak current capability was also tested. The peak current as high as 9.2 A was extracted. There were no indications of the surface charge limit, and the charge output was limited by the laser energy. This is the first demonstration that the NLC compatible beam with polarization approaching 80% is achievable.

REFERENCE

- [1] [www-project.slac.stanford.edu/lc/local/Reviews/Apr2001/Electron Sources including e- Booster v2.pdf](http://www-project.slac.stanford.edu/lc/local/Reviews/Apr2001/Electron%20Sources%20including%20e-Booster%20v2.pdf)
- [2] G.A. Mulhollan, A.V. Subashiev, J.E. Clendenin, E.L. Garwin, R.E. Kirby, T. Maruyama, and R. Prepost, SLAC-PUB-8753, Phys. Lett. A282, 309 (2001).
- [3] K. Togawa et al, Nucl. Instrum. Methods A414, 431 (1998), and T. Maruyama PPRC-TN-00-2.

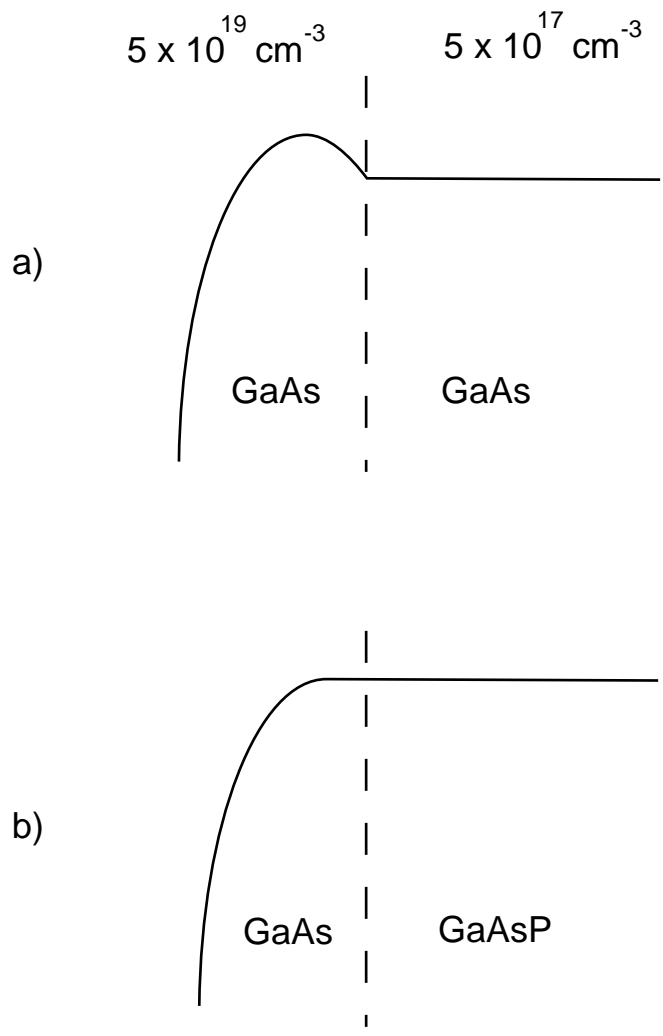


Figure 1 Conduction band for (a) strained GaAs and (b) strained GaAsP

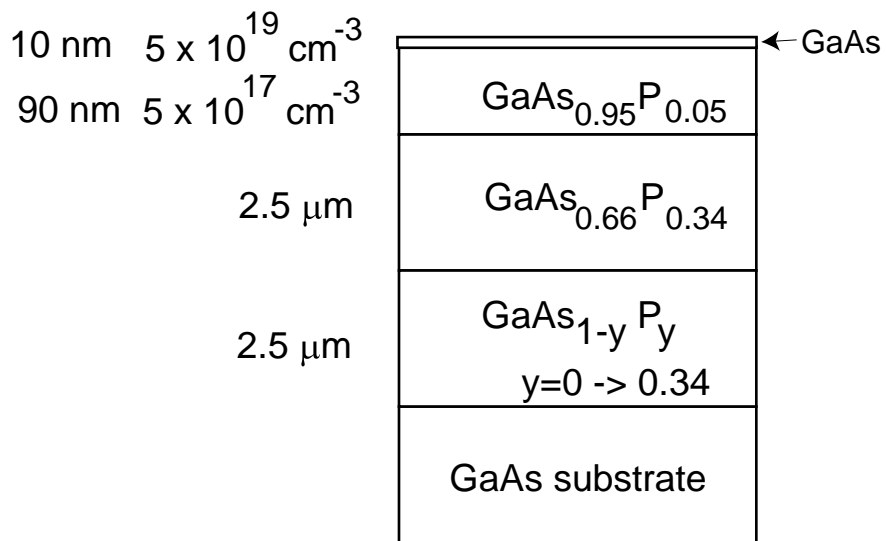


Figure 2 High-Gradient-Doped Strained GaAsP

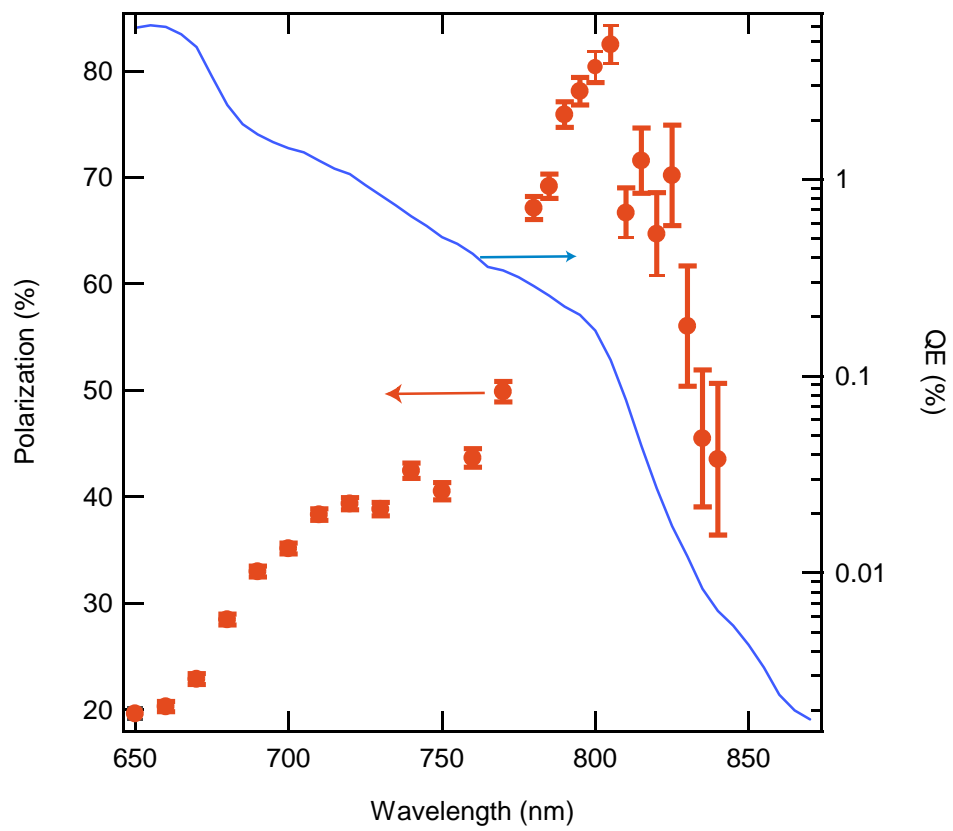


Figure 3 Polarization and QE as a function of wavelength measured in the CTS lab.

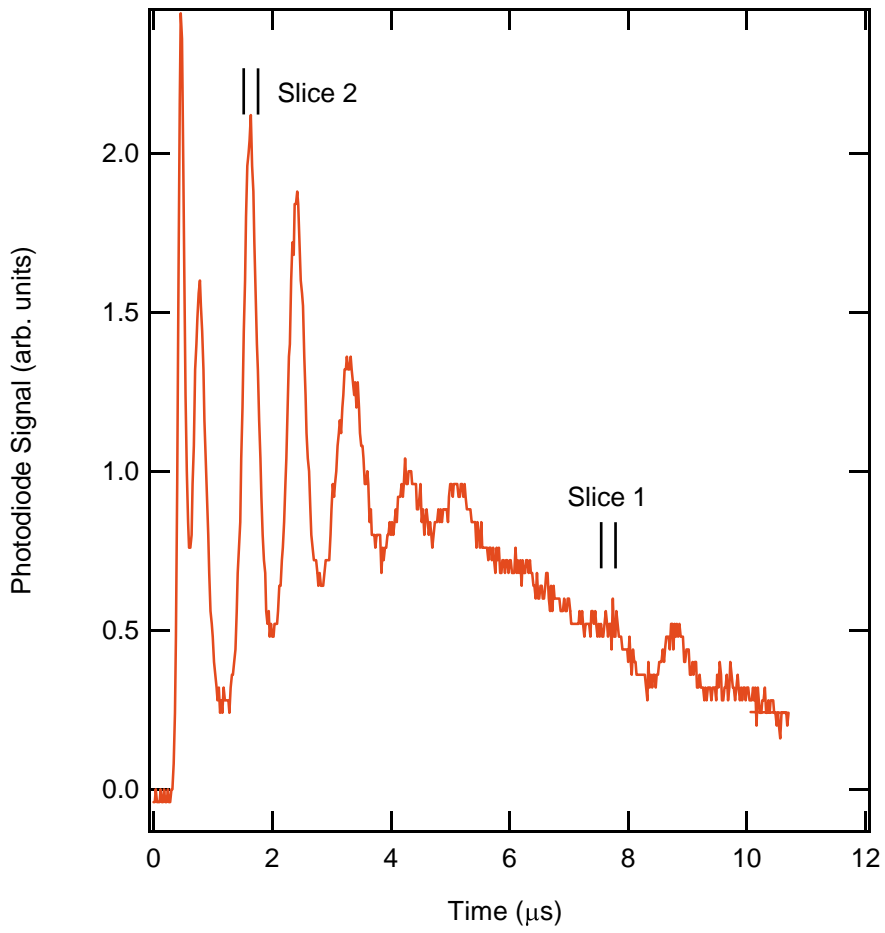


Figure 4 Flash-Ti laser pulse before slice.

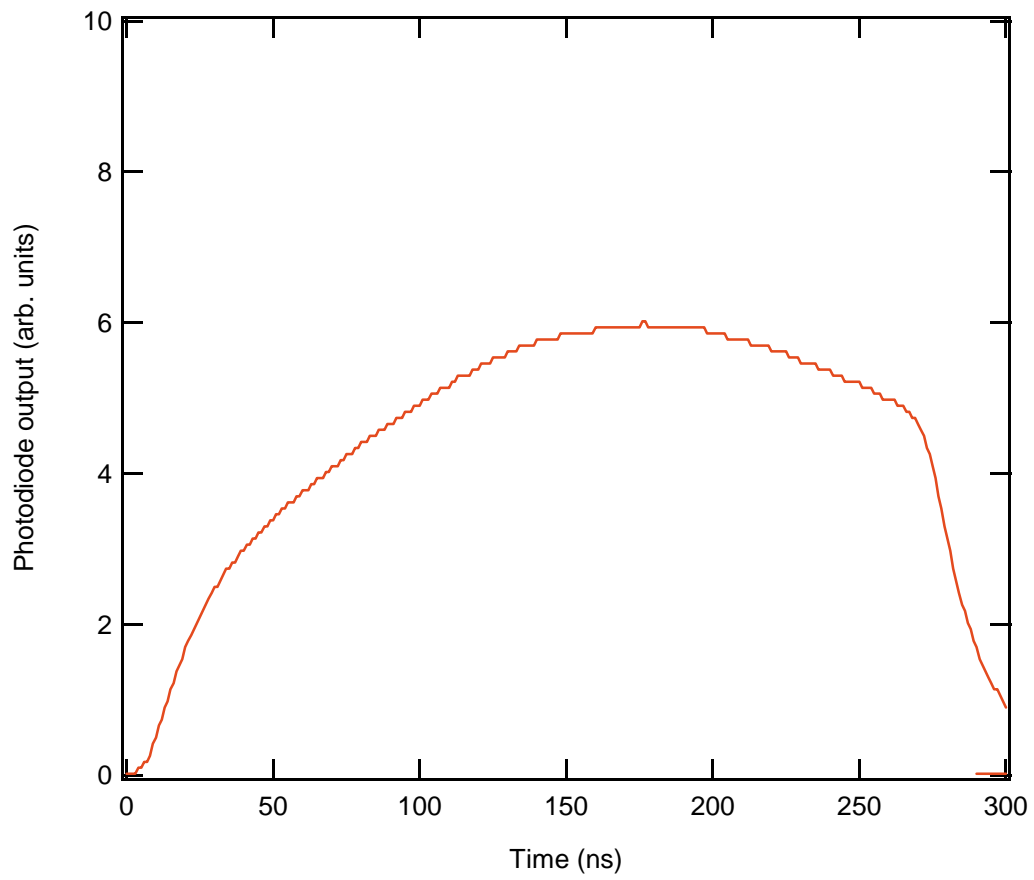


Figure 5 Flash-Ti laser pulse

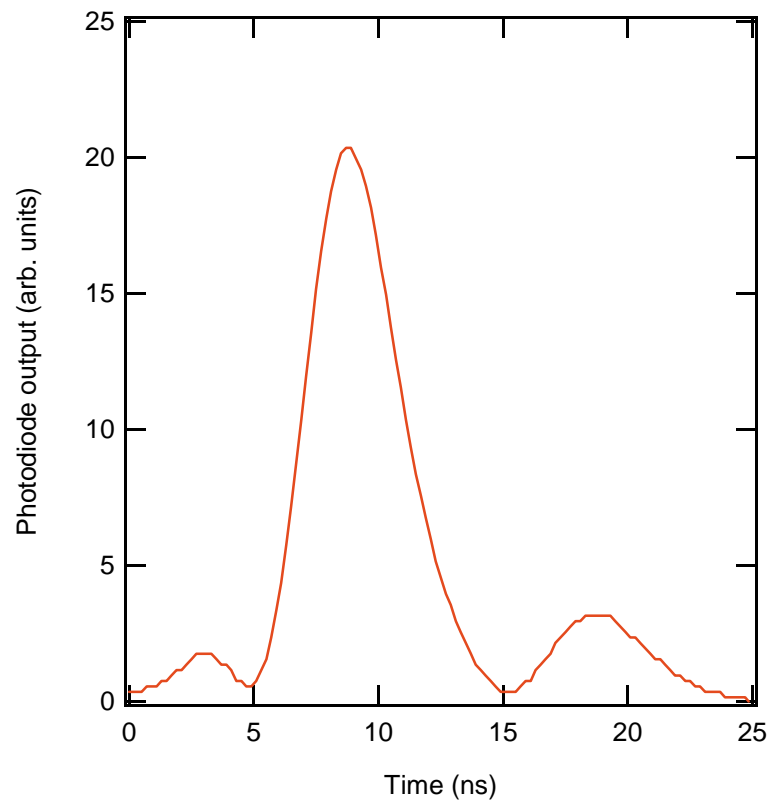
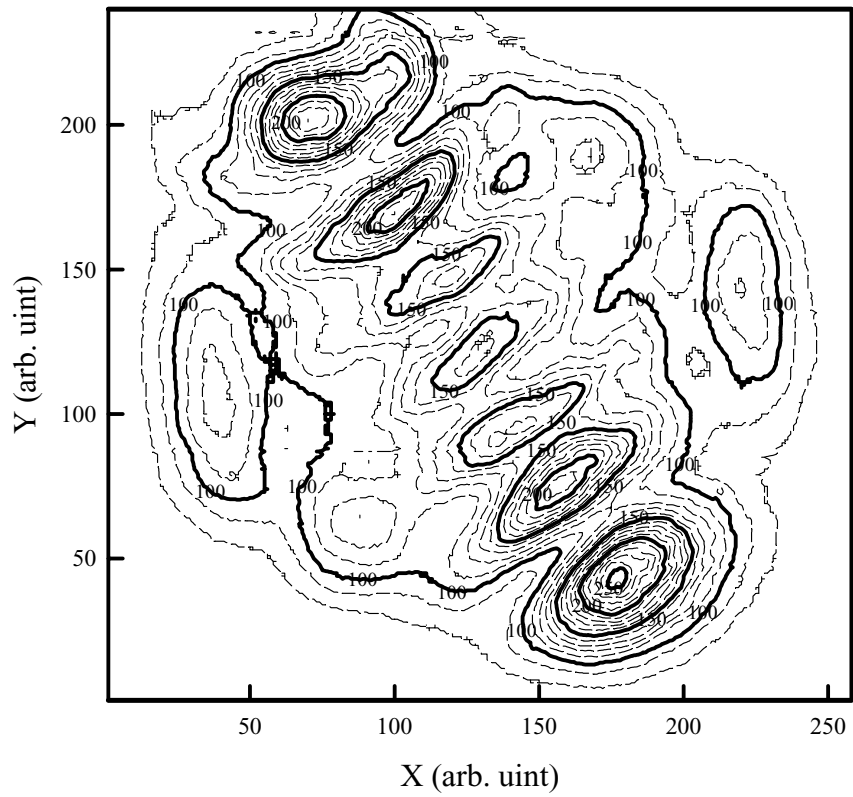


Figure 6 YAG-Ti laser pulse

a)



b)

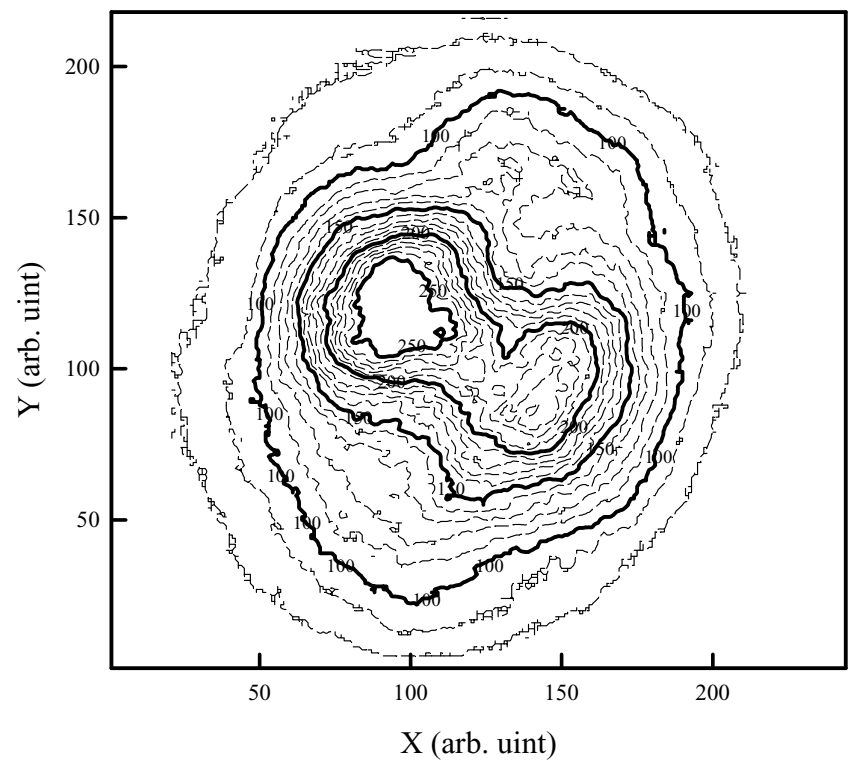


Figure 7 Laser beam profile a) Flash-Ti, and b) YAG-Ti

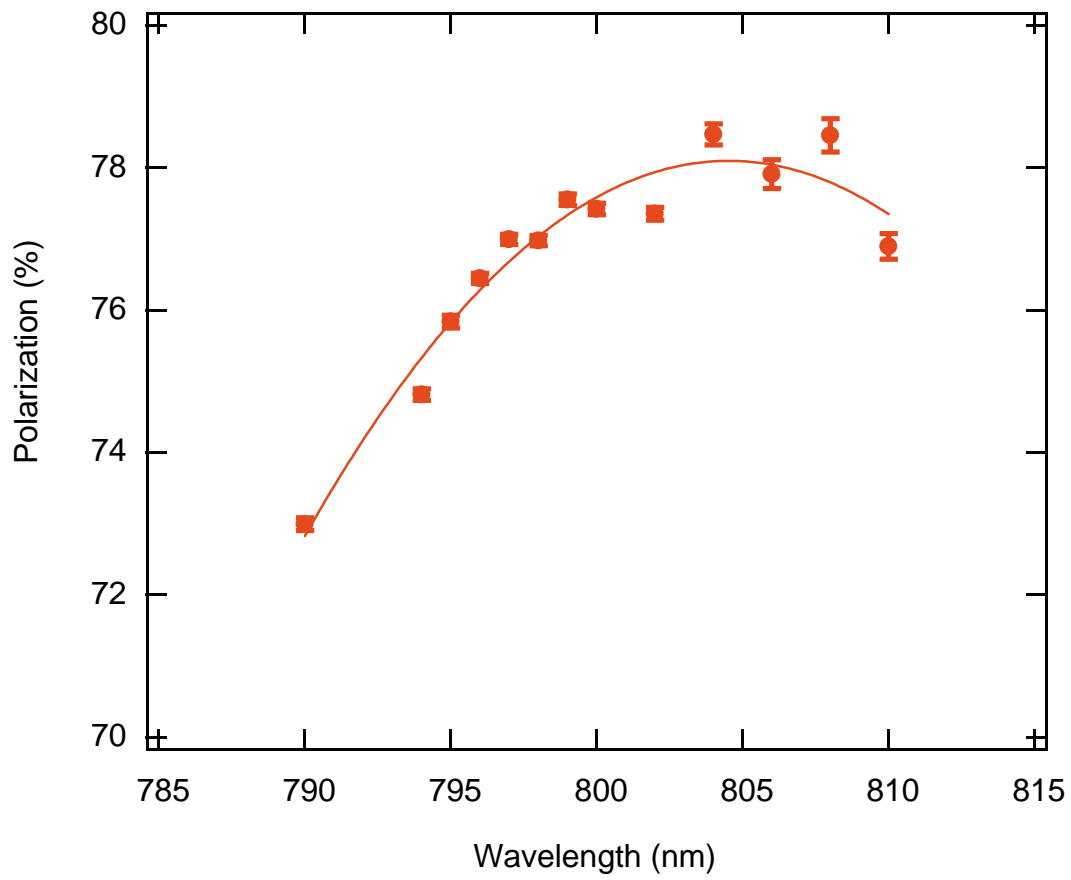


Figure 8 Polarization as a function of wavelength measured at 120 KV.

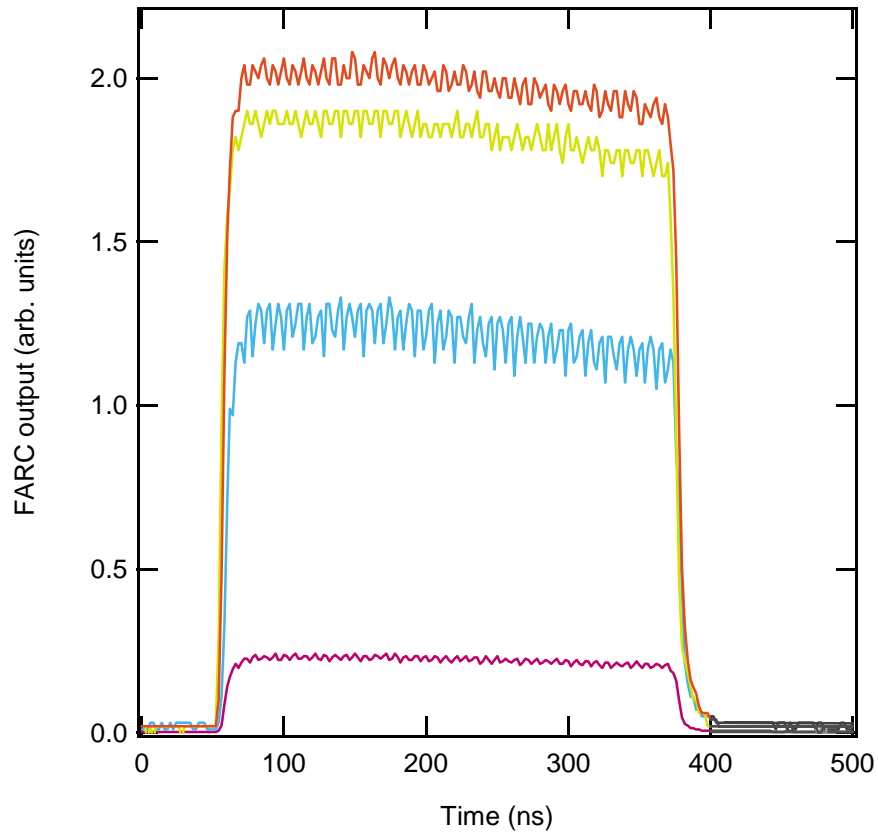


Figure 9 Faraday cup signal measured using varying Flash-Ti laser energies.

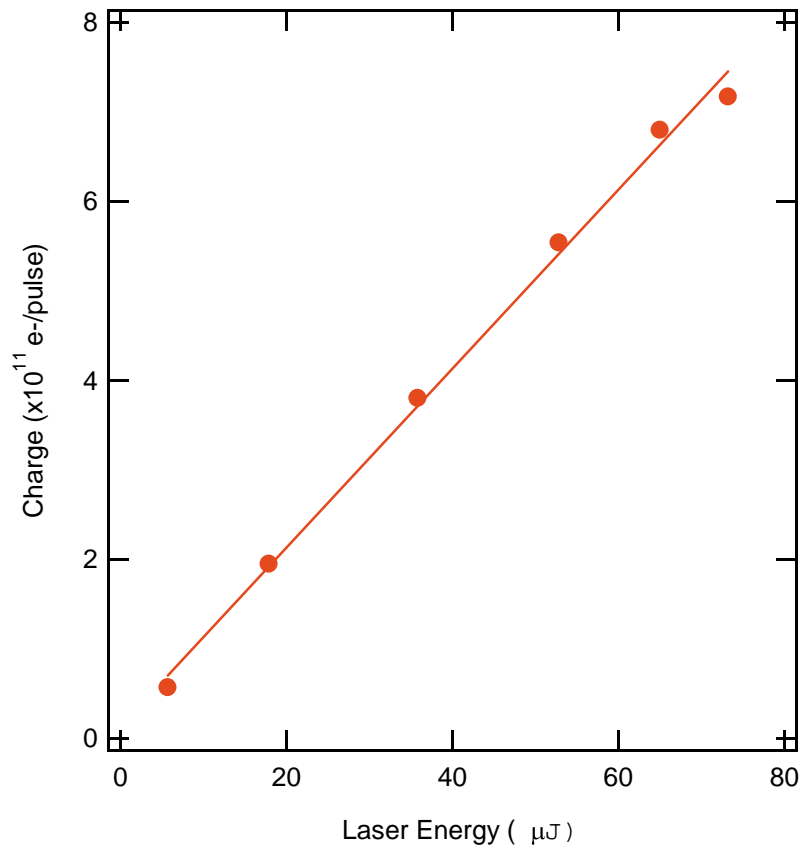


Figure 10 Charge output as a function of Flash-Ti laser energy.

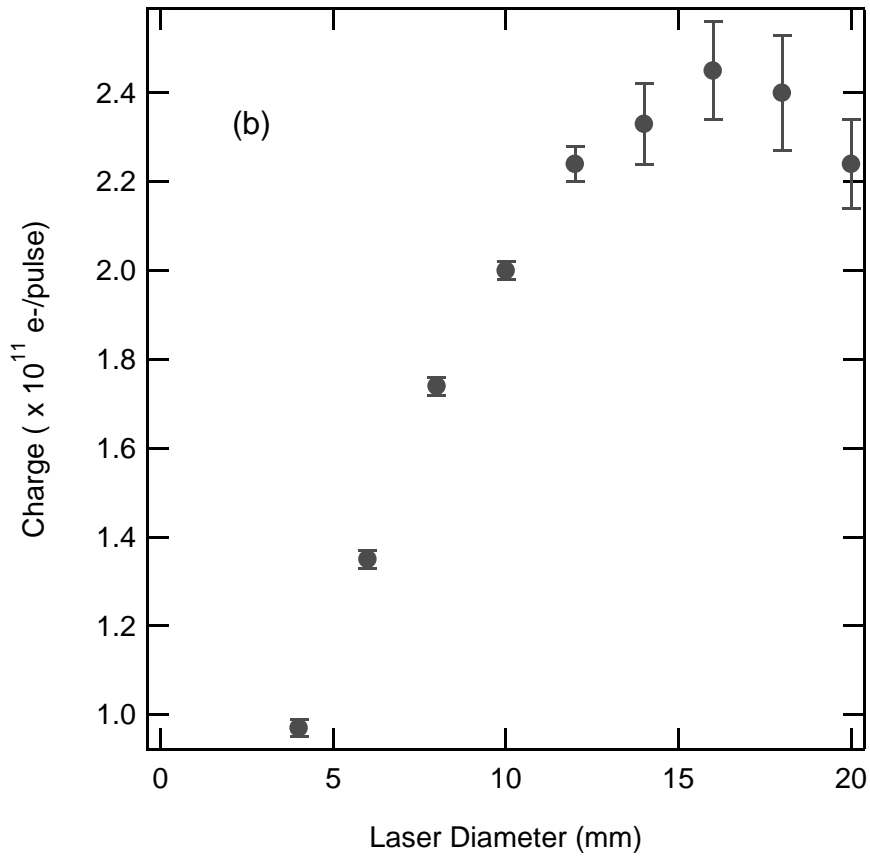
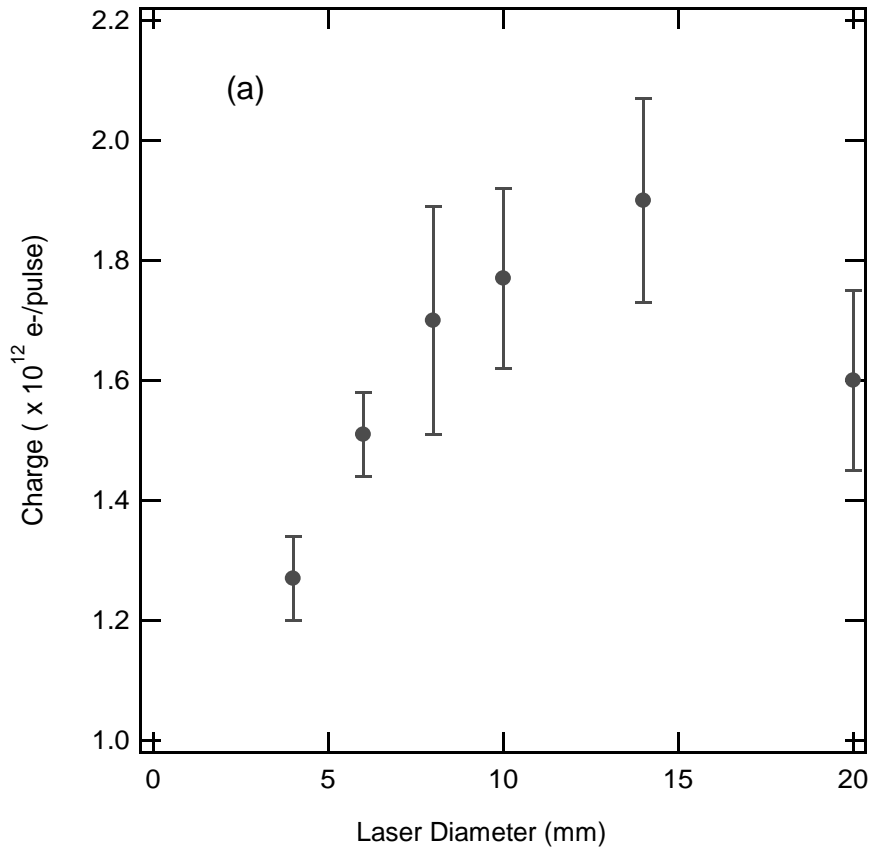


Figure 11 Charge output as a function of laser beam diameter.
(a) Flash-Ti, and (b) YAG-Ti laser.

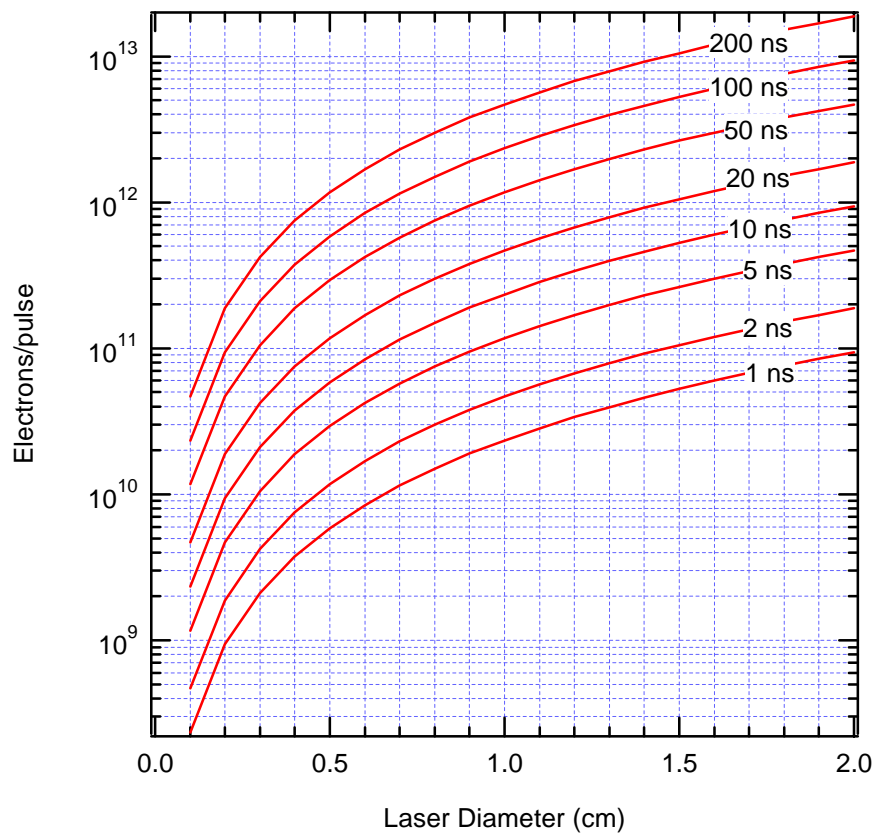


Figure 12 Space-Charge-Limited Photoemission

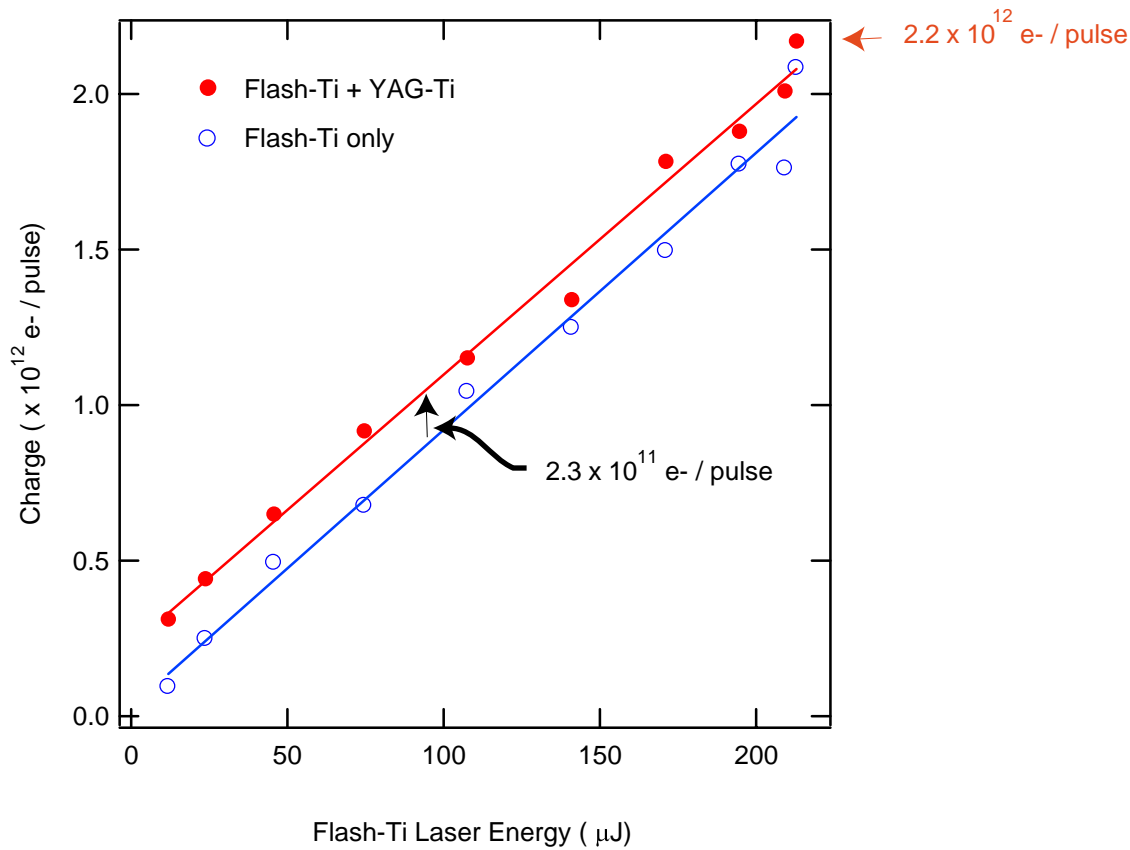


Figure 13 Charge output as a function of the Flash-Ti laser energy.